Development of a 4 MW Full-Size Wind-Turbine Test Bench

Nurhan Rizqy Averous[1,2], Marco Stieneker[1,2], Stefan Kock[1,3], Cristian Andrei[1,4], Alexander Helmedag[1,5], Rik W. De Doncker[1,2], Kay Hameyer[1,4], Georg Jacobs[1,3], Antonello Monti[1,5]
[1]Center for Wind Power Drives, RWTH Aachen University, Aachen, Germany
[2]Institute for Power Generation and Storage Systems, E.ON ERC, RWTH Aachen University, Aachen, Germany
[3]Chair for Wind Power Drives, RWTH Aachen University, Aachen, Germany
[4]Institute for Electrical Machines, RWTH Aachen University, Aachen, Germany
[5]Institute for Automation of Complex Power Systems, E.ON ERC, RWTH Aachen University, Aachen, Germany

***Abstract*—The in-field validation of wind turbines behavior is very time consuming and cost intensive, especially when fault ride-through (FRT) tests are conducted. Full-size wind-turbine test benches allow a realistic operation of wind turbines in an artificial environment. Due to the independency of wind and grid conditions, the cost and duration of the test program and certification can be reduced. This paper presents the development of 4 MW full-size wind-turbine test bench following a multi-physics hardware in-the-loop (HiL) concept. With the currently installed test bench setup, a synchronization of the device-under-test converters is possible. Through the measurement results of the test programs conducted on the test bench, the capability of the test bench in replicating the field conditions is demonstrated. In addition, a time consuming efficiency measurement can be performed with the reduced duration on the test bench. This shows another main benefit of the test bench compared to the conventional test method for wind turbines.**

I. Introduction

The contribution of wind energy to the world's energy mix was steadily increasing during the last decades. Due to the depletion of fossil energy, its share is expected to rise further in the future. As a consequence, the security of energy supply will strongly rely on the performance of wind turbines. Hence, not only the efficiency to ensure the economic operation of wind turbines is highly important. The wind turbines are also required to offer a high reliability for minimizing the downtime and loss of power generation. It is also necessary, that the wind turbine is able to support the grid stability during failures.

These aspects have to be considered when designing a new wind turbine system. However, after the development process, test and certification procedures have to be conducted to ensure a successful product deployment. Since in-field testing and certification depend on wind and grid conditions, a system test bench accelerates the process of product deployment considerably. Also in contrast to in-field tests, the reproducibility of measurements is given.

Furthermore, the laboratory environment allows the installation of additional measurement points that enable a more advanced and more detailed characterization of the wind turbine nacelle. Hence, test benches for wind turbine systems offer a more effective and efficient method to accomplish the design validation of wind turbines (WT).

At the Center for Wind Power Drives (CWD) at RWTH Aachen University, a 4 MW full-size wind-turbine test bench has been built for conducting comprehensive studies on wind turbine nacelles. The implemented multi-physics hardware-in-the-loop (HiL) concept reproduces realistic stresses on the device-under-test (DUT) as it would experience in the field. The mechanical stress caused by the wind field is emulated as well as the electrical interaction of the DUT with the grid. Furthermore, critical test scenarios such as fault ride-through (FRT) tests can be performed consuming less time and cost. The concept has already been validated with a 1 MW test bench developed at RWTH Aachen University [1].

This paper presents the newly developed 4 MW full-size wind turbine test bench. The construction of test bench is discussed followed by the details about the DUT. Before demonstrating the test results, the measured emulated grid -voltage profile as well as the influence on the DUT are presented and discussed. Afterwards, the application of the some possible load scenarios for the DUT is demonstrated. Furthermore, an efficiency measurement that can also be conducted on the test bench finalizes the demonstration of the test bench capabilities before conclusions are drawn.

II. Test Bench Construction

The schematic of the developed 4 MW full-size wind-turbine test bench is given in Fig. 1. A medium-voltage (MV) active-front-end (AFE) converter links the test bench to the 10 kV public ac grid and ensures simultaneously a constant voltage of 5 kV at the dc bus. An MV power electronics converter connected to the 5 kV dc bus drives the 4 MW direct-drive permanent-magnet (DDPM) motor. Due to the direct-drive concept, a gearbox to adapt the rotational speed is not required. Hence the DDPM is directly coupled to the rotor hub of the DUT. The mechanical coupling includes a non-torque loading (NTL) unit that is used to emulate forces on the shaft caused by the rotor operating in realistic wind fields.

The electrical energy generated by the DUT is fed into the emulated grid. The voltage of the point of common-coupling (PCC) with the artificial grid is 20 kV. The ac voltage at the PCC is emulated by a MV grid emulator with a current power rating of 3.5 MVA. However, this power rating will be increased up to 17 MVA in the next step to allow the emulation of severe grid faults. Currently, the power capability of the grid emulator has been adjusted to minimize the size of the overall passive elements while still facilitating the tests

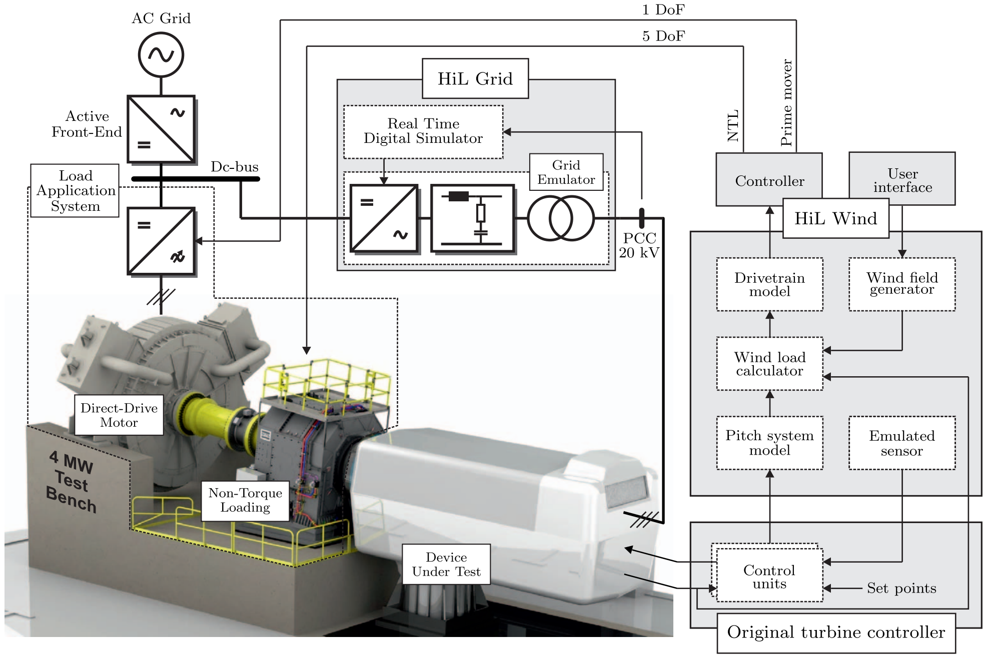

Fig. 1. Schematic of the 4 MW full-size wind-turbine test bench

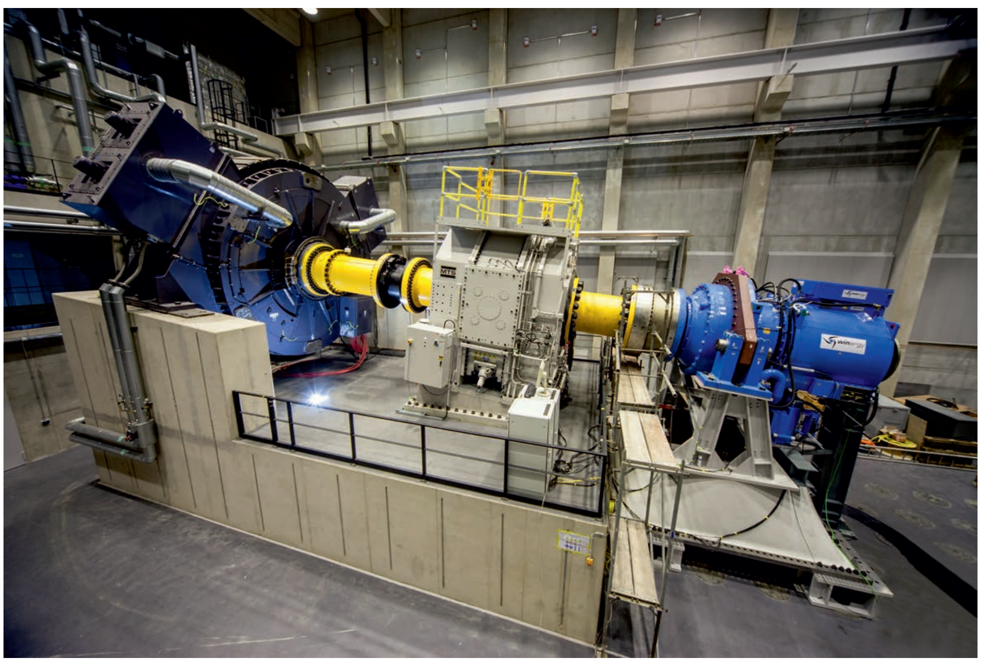

Fig. 2. Photography of the 4 MW test bench

of the currently installed device-under-test setup. The grid emulator is connected to the same dc-link feeding the power electronic converter that drives the DDPM. Hence, the power flow circulates within the test bench and only the losses have to be compensated by AFE connected to the grid.

A. Wind Load Emulator

The wind load emulator is part of the multi-physical HiL environment that represents the physical rotor hub interfaces. It includes a real-time simulation of the aerodynamic and mechanical characteristics of the rotor as well as a load application system (LAS) to apply forces and moments to the DUT.

Simulation Process: The aerodynamic simulation comprises two separate processes. The first process is responsible for the generation of a stochastic 3D wind-field that is based on the average wind speed and turbulence intensity at discrete sections of the rotor plane. The second process calculates the resulting forces and moments at the virtual load application point in the center of the rotor hub as a function of wind direction, measured rotational speed and pitch angle. Afterwards the calculated forces and moments are forwarded as reference values to the LAS.

Load Application Process: The LAS can be divided into two parts. The first part is responsible for the distribution of the simulated torque to the main shaft of the test drive train which is realized by the DDPM motor. It is capable of delivering torque of up to $2.7\,\mathrm{MNm}$. The direct-drive prime-mover concept leads to improved torque transmissibility, controllability and dynamic behavior of the test drive-train compared to the concept in [1]. The second part applies the calculated forces and bending moments by means of an NTL unit. It consists of a support frame and 6 pairs of pre-stressed actuators that are located on a spinning journal bearing disc and a radial bushing. With the NTL unit in the test setup it is possible to apply the load in all 6 degree-of-freedom (DoF) and to realize maximum bending moments of about 7 2MNm. During uniaxial performance the LAS supports a thrust force up to $4\,\mathrm{MN}$ in addition to radial and vertical forces of about $3.25\,\mathrm{MN}$.

B. Grid Emulator

The grid emulation can be split-up into two tasks. First, a model of the electrical grid has to be implemented within a real-time simulation environment that allows the HiL setup. Second, the simulated behaviors of the power grid has to be mapped to power level with a power interface. The power interface is realized with the MV power electronic converter setup that emulates the behavior of the PCC. The input to the control of the power converter is the signal-level output of the grid simulation. In Fig. 1 the topology of the converter setup is presented. A MV power electronic converter based on a three-level neutral-point-clamped (3L-NPC) topology [2] is utilized to provide a $50\,\mathrm{Hz}$ $3.1\,\mathrm{kV}$ voltage at its terminal.

A three-phase LC-filter with passive damping is installed to mitigate the voltage harmonics caused by the switching of the converter. Its resonance frequency is tuned at $f_{\mathrm{res}} = 627\,\mathrm{Hz}$ in order to obtain a total harmonic distortion (THD) of the PCC voltage lower than $8\,\%$. This THD level already complies with the specification in the standard DIN EN 50160 [3] describing the maximum values wind turbines have to deal with. Finally, a transformer rated to $7\,\mathrm{MVA}$ steps the voltage up to $20\,\mathrm{kV}$ at the PCC.

The grid simulation is realized with a Real-Time Digital Simulator (RTDS) modeling the behavior of the electrical power grid at the PCC. The grid model allows the simulation of different operational states of the power grid. Hence, the operation behavior of DUTs can be investigated under various grid conditions. That includes normal operation points as well as faulty states. The RTDS therefore builds the simulation part of the electrical HiL setup.

The simulation of the grid has to be conducted in real time as it is necessary for the HiL setup. For mapping all relevant dynamics of the electrical network, the time step of the simulation is chosen to be $50\,\mathrm{\mu s}$. This implies the need for a high performance characteristics of the simulation hardware. The RTDS is a highly-parallel simulation environment specialized on electrical grids simulations.

Next to the need for real-time simulation, the signal interface between RTDS and the power converter has to be operated in real time. This means it has to be deterministic with a low latency communication setup. As a result from the small simulation time-step the latency of the communication link has to be within μs range maximum. In order to minimize the interference caused by the high-power converter environment a digital connection was chosen. Due to the use of the Ethercat protocol, all of the demands on the communication between the RTDS and the power-converter control is fulfilled.

A real-time simulation of the power grid implies the advantage that different kinds of power grids can be modeled. This supports the investigation of the wind turbines at any type of PCC connection e.g. weak or strong power grids. In addition to certification the combination of power electronics for the HiL interface and the real-time simulation of the power grid helps with research and the design process itself for any relevant type of the grid connection of wind turbines.

FRT Tests define a subset of possible grid faults which can be realized with a power electronic converter setup as well. This way, certification of grid code conform behavior of the wind turbine can be proven. Certification on test benches implies significant advantages as there is not any dependency on the outer weather situation as it is the case in an in-field test. Moreover, the testing procedures are repeatable.

III. Device-Under-Test

The DUT that is shown in Fig. 3(a) is integrated into the setup on the $4\,\mathrm{MW}$ test bench as depicted in Fig. 2. It is a highly integrated gearbox-generator unit named HybridDrive manufactured by Winergy [4]. The HybridDrive consists of a two-stage planetary gearbox directly coupled to a medium-speed permanent-magnet synchronous generator enclosed within the same housing. However, the generator of the HybridDrive has three electrically isolated three-phase winding systems. The main characteristics of the Winergy's HybridDrive are given in Table I.

Since the frequency of the generator's output voltage depends on the rotational speed of the shaft, a power electronic

(a) Winergy's HybridDrive

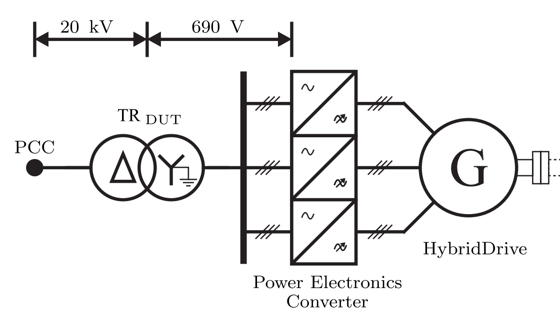

(b) Power electronics converters

Fig. 3. Device under test (DUT)

TABLE I. MAIN CHARACTERISTICS OF THE WINERGY'S HYBRIDDRIVE

Max. input torque	2549 kNm
Rated speed on high-speed shaft	431 rpm
Gearbox transmission ratio	$i = 35$
Rated electrical frequency	86.2 Hz
Electrical output power	3.12 MW
Rated voltage	720 V

converter is applied for the grid connection. Each three-phase system of the HybridDrive generator is connected to an individual frequency converter. On the grid side, these power electronic converters are connected to a transformer that steps the output voltage of 690 V up to the PCC voltage of 20 kV. The transformer is rated for 3.5 MV A and provides a leakage inductance of 7.5 %. Power capacity overload is detected by the frequency converter. In case of exceeding the maximum operation temperature, the DUT and the test bench will be shut down automatically.

IV. GRID SYNCHRONIZATION OF THE DUT

An important aspect regarding the development of the test bench is that the DUT has to synchronize with the emulated electrical grid at the PCC. Also, any negative impacts to the DUT as a result of the construction of the grid emulator have to be ensured minimum. In the following, the emulated grid-voltage profile at the PCC during no-load operation will be assessed. Afterwards, the characteristic of the measured power quality during static operation is analyzed to investigate eventually interactions between the grid emulator and the DUT.

A. Emulated Grid-Voltage Quality

During the commissioning, the quality of the emulated grid under no-load condition is in the focus to ensure the grid synchronization of the DUT at the PCC. Besides, assessing the quality of the grid voltage under no-load condition improves the characterization of the DUT during operation. Hence, the contribution of the DUT and grid emulator at the PCC can be distinguished. The measured profile of the grid voltage is assessed by comparing with the recently valid standards.

The DUT monitors the grid voltage on the 690 V level and evaluates voltage quality before connecting to the artificial grid. Fig. 4(a) shows the measured three-phase voltage on the 690 V side of the DUT transformer between the line and neutral point of the transformer. As shown in this figure, the grid emulator setup is capable of replicating a three-phase 50 Hz grid voltage with a relatively low harmonic content although it is emulated by means of a converter system.

To obtain a better information about the harmonic content in the emulated grid-voltage, a Fast-Fourier Transformation (FFT) can be applied to the voltage curve in Fig. 4(a). The FFT transforms the time domain waveform of the voltage into the frequency domain to obtain the harmonic content. Additionally, the information about the harmonic content allows the calculation of the total harmonic distortion (THD) using (1) [3]. The calculation is based on the geometrical summation of the amplitude of the voltage harmonics V_h normalized to the amplitude of the fundamental voltage V_1.

$$\mathrm{THD}_V = \frac{\sqrt{\sum_{h=2}^{50} |V_h|^2}}{V_1} \times 100\,\% \qquad (1)$$

(1) considers only the harmonic frequencies between 100 Hz and 2500 Hz for a 50 Hz power system. It gives a harmonic order (h) range between 2 and 50. For the THD calculation, the standard EN 50160 considers a harmonic order range only up to 40^{th} order. However, the guideline for grid compliance tests in the standard IEC 61400-21 [5] requires the voltage harmonics to be assessed up to the 50^{th} order. Compared to the standard EN 50160, the IEC 61400-21 gives the more critical restriction.

Figure 4(b) shows the frequency spectrum of the phase u voltage. The calculated THD is about 4.95 %. This THD value already complies with the standard EN 50160 and IEC 61400-21. The maximum THD level according to the standard EN 50160 is 8 %. The standard IEC 61400-21 limits the maximum THD of the voltage to 5 % for grid compliance tests of wind turbines.

The frequency spectrum of the voltage in Fig. 4(b) proves the low harmonic content in the grid voltage. It can be seen from this figure that the designed LC-filter for the grid emulator reduces the voltage harmonics due to switching of the grid emulator converter. This means that the emulated grid-voltage on the developed test bench already represents a realistic grid voltage in terms of the voltage quality.

TABLE II. PROFILE OF THE EMULATED GRID-VOLTAGE

Parameter	Measurement	Reference	Evaluation
RMS voltage	687.4 V	690 V ± 10 %	ok
Frequency	49.99 Hz	50 Hz ± 0.5 Hz	ok
THD	4.92 %	< 5 %	ok
Unbalance factor	0.3 %	< 2 %	ok

Beside the voltage quality, other parameters that describe the profile of the grid voltage have to be assessed before connection of the DUT. Table II summarizes the voltage profiles of the emulated grid-voltage as well as the comparison with the recently valid standards. In addition to the THD that has been previously discussed, the root mean square (RMS), the frequency and the unbalanced factor are presented in the Table II. The measured values presented in the table are the average values over ten fundamental cycles.

Similar to the THD, all parameters in Table II are assessed referring to the standard IEC 61400-21. As it can be seen, the profile of the emulated grid-voltage fulfills the criteria. Such a voltage profile ensures the grid synchronization of the DUT with the emulated grid. Additionally, the grid emulator does not generate any excessive voltage unbalance that may also distort the operation of the DUT.

B. Operation of the DUT

The test bench has been commissioned up to the nominal power of the HybridDrive generator. The commissioning aims the operation of the DUT with the emulated grid and the recuperation of the generated electrical energy into the artificial

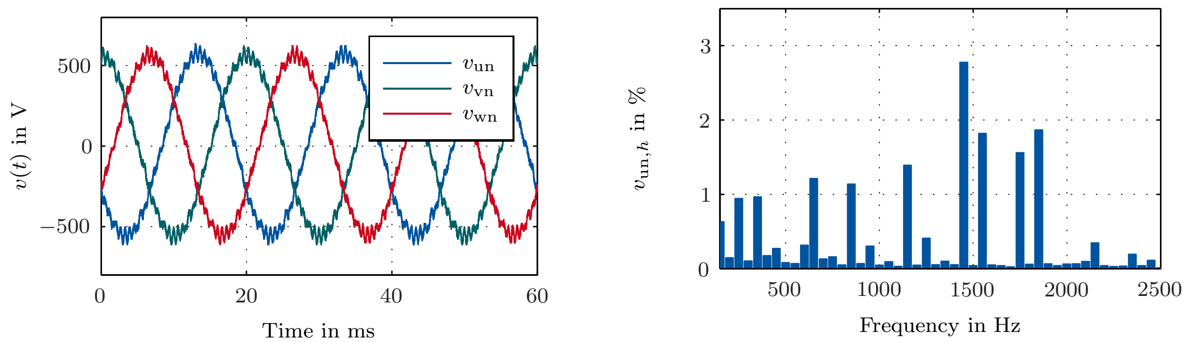

(a) Instantaneous waveform

(b) Frequency spectrum

Fig. 4. Measured emulated grid-voltage

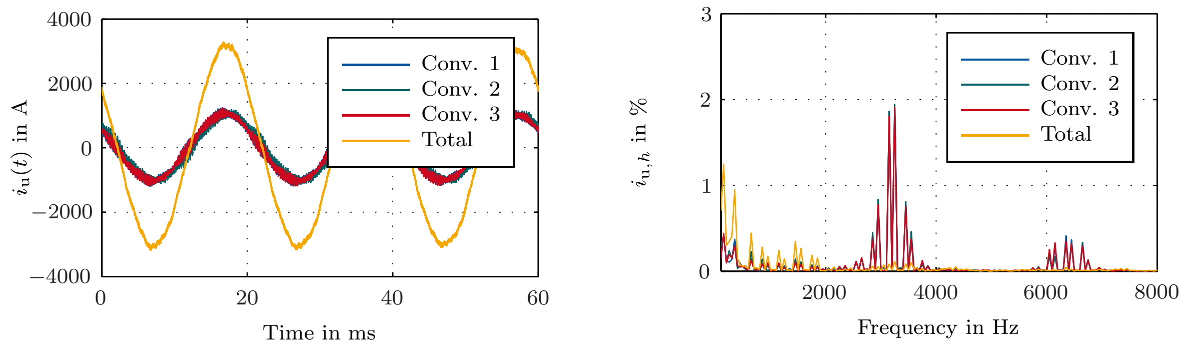

(a) Instantaneous waveform

(b) Frequency spectrum

Fig. 5. Measured phase current on the low-voltage side of the DUT transformer

grid. During the commissioning, the basic functionality of a wind turbine drive train where the DUT converters regulate the load torque on the drive-train shaft was also tested.

Figure 5 shows that the emulated grid-voltage contains harmonics where the highest magnitudes appear between $1\,\mathrm{kHz}$ and $2\,\mathrm{kHz}$. These voltage harmonics may result in a harmonic distortion in the DUT current once it is in operation. To further examine the influence of the voltage harmonics, the phase current of all of the individual DUT converters as well as the total current flowing into the grid are recorded as depicted in Fig. 5. The measurement is taken with a generator power of about $2.67\,\mathrm{MW}$.

Additionally, the frequency spectrum of the captured current waveforms are also obtained as shown in Fig. 5(b). Within the frequency range between $1\,\mathrm{kHz}$ and $2\,\mathrm{kHz}$ where the voltage harmonics with the highest amplitudes exist, no significant harmonic distortion in the total DUT current (orange curve) can be observed. The THD of the DUT current within this frequency range is below $0.35\,\%$. This means that the emulated grid-voltage has a negligible impact on the DUT during operation.

As shown in Fig. 5, all DUT converters feed current harmonics into the emulated grid with frequencies around the switching frequency. Their magnitudes almost reach $2\,\%$ of the fundamental current. The current harmonics with such a characteristic are mainly caused by the switching operation of the DUT converter. Even so, these current harmonics compensate each other at the collection point of the converters due to the interleaved switching strategy implemented in the DUT converters. Such an operation helps minimizing injected current harmonics into the grid to fulfill the grid requirements keeping the size of the filter on a minimum.

V. Reproduction of the Field Load Cases

A. *Mechanical loads*

Due to the stochastic and unsteady wind conditions, wind turbines in the field are exposed to very heavy and highly fluctuating wind loads in all six degrees of freedom (6DOF). The ability to measure the local load conditions caused by wind loads offers in return the potential to improve the design process of wind turbine gearboxes and generators by reducing the design uncertainties. The influence of these 6DOF wind loads on the local loads in a wind turbine gearbox is analyzed in the first measurements on the $4\,\mathrm{MW}$ wind turbine system test bench.

The DUT is mounted on the test bench similarly to the field operation via elastomeric elements at the gearbox input flange as well as in the bushings at the torque arm of the DUT housing. This type of mounting ensures a realistic displacement behavior of the DUT relative to the test bench frame during operation. Moreover this mounting concept reduces the occurrence of parasitic forces resulting from the unavoidable geometrical deviations in the assembly of the DUT and the deformation of the test bench frame.

For the measurement of the displacement behavior of the system, the axial-, radial- and angular displacements of the gearbox input flange are measured. In addition to this the bushings at the torque arms of the DUT are equipped with a displacement sensors to measure the DUT displacement

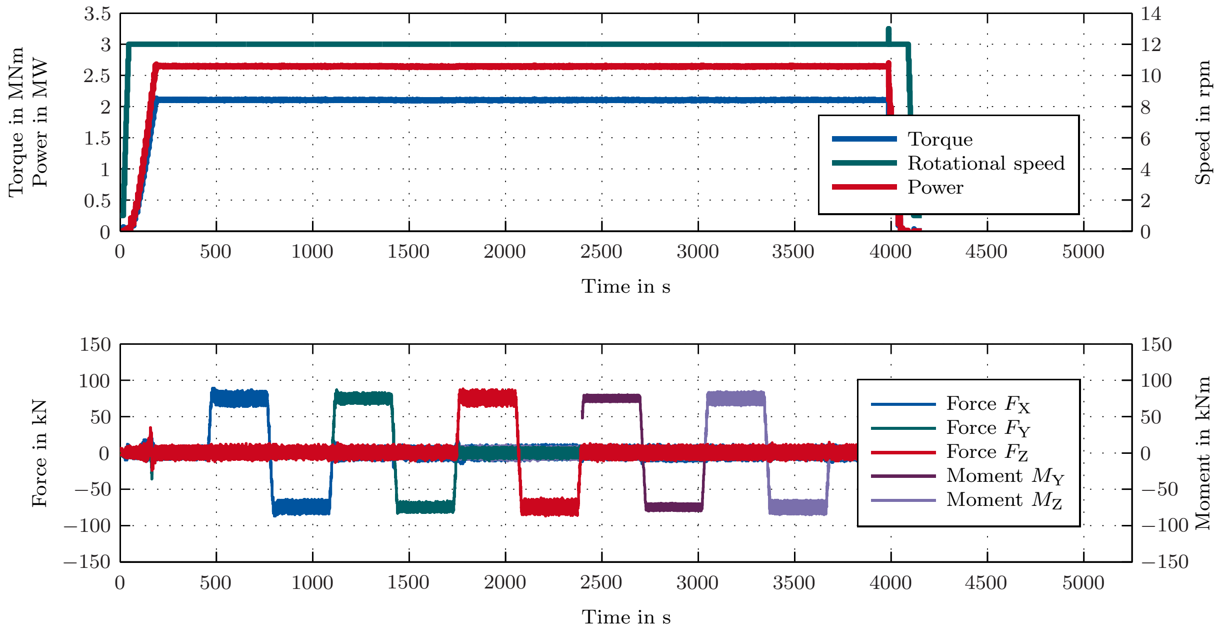

Fig. 6. Forces and moments during test program

relative to the test bench frame. Moreover the ring gears and the sun gears of both planetary gearbox stages are equipped with strain gauges in the tooth roots to determine the impact of gearbox input loads on the local loads in the teeth contact of the DUT. For the analysis of the 6DOF wind loads influence, a test program that includes varied forces and bending moments under constant rotational speed and torque is used. An example of the test procedure is shown in Fig. 6.

The measurement results show, that the displacement behavior of the DUT depends strongly on the torque level of the drivetrain. For operation points with low torque multi-axis displacements can be observed. This effect can be attributed to the low pretension of the elastomeric elements. Tests with increased torque result in single-axis displacement with decreased relative amplitudes based on the additional gearbox input loads. For example, the application of a single radial load in z-direction leads at maximum torque to a pure angular displacement through the y-axis. At $20\,\%$ torque the relative displacement based on the z-force is nearly doubled. In addition to this a multi-axis angular displacement through the y- and z-axis can be observed. The analysis of the tooth root stress has shown, that gearbox input loads are affected strongly by the additional 5DOF forces and moments at the gearbox input flange. Therefore it is very important to use a drivetrain suspension concept which is able to create a pure torque load situation for the gearbox at all torque levels.

The possibility to analyze the capability of the main bearing and gearbox suspension system to reduce reaction forces at the gearbox input is another strong advantage of a system test bench which shows the great potential like the $4\,\mathrm{MW}$ wind-turbine system test bench at the CWD.

B. Grid faults

The high penetration of wind energy into the power grid forces modern wind turbines to contribute more in maintaining the power system stability and the security of energy supply. Unlike conventional wind turbines that are allowed to disconnect from the grid in case of grid faults, modern wind turbines have to ride through them without disconnecting from the grid [6]. On the one hand, this prevents a massive loss of energy. On the other hand, such operation strategies (FRT) may result in a severe component stress. In addition, some grid codes have even extended the requirements for the wind turbines behavior such that the injected reactive current has to be increased particularly during grid faults to maintain the grid voltage level [7].

Such significant extensions in the grid codes have forced the design concept of wind turbines to a higher level. Besides testing of the developed system it is also very crucial to check if the requirements mentioned above are fulfilled. The key to obtain sophisticated test results is the realistic replication of the voltage dips during grid faults.

The international standard IEC 61400-21 provides a guideline to perform the so-called fault ride-through (FRT) tests. According to the standard, the grid compliance test program must cover symmetrical as well as unsymmetrical faults. In the following, the test results demonstrating the emulation of grid faults on the test bench are shown and analyzed.

In Fig. 7, the voltage waveforms on the low-voltage (LV) side of the DUT transformer during grid-fault events are shown. The waveform of an $80\,\%$ symmetrical voltage dip is depicted in Fig. 7(a). As shown in this figure, all three-phase voltages drop down symmetrically. Due to the symmetrical behavior, neither negative nor zero-sequence voltages are generated. Hence, only the amplitude of the voltages at the PCC and at the terminal of grid emulator are affected while the phases remain unchanged.

Unlike in symmetrical fault cases, the phases of the emulated voltages are affected by the transformer configuration in case of unsymmetrical faults. In Fig. 7(b), an unsymmetrical fault with $90\,\%$ positive-sequence voltage and $10\,\%$ negative-sequence voltage is shown. Similar to the symmetrical fault

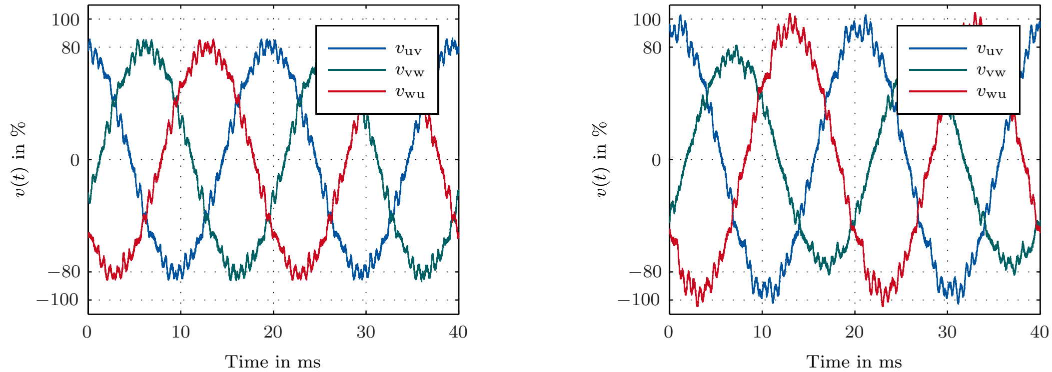

(a) Symmetrical fault (b) Unsymmetrical fault

Fig. 7. Emulated grid faults

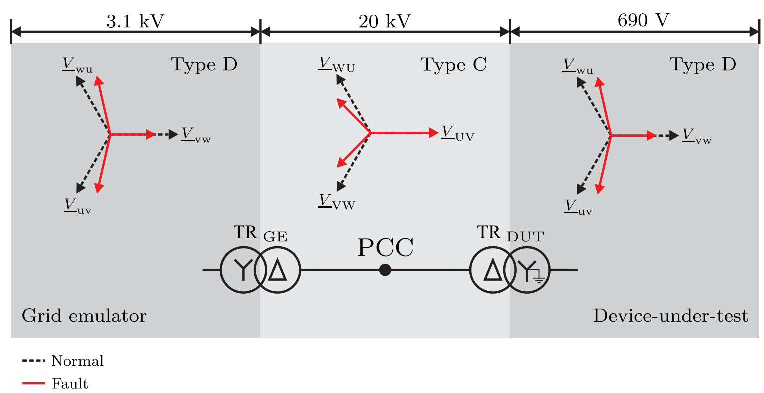

Fig. 8. Propagation of fault-voltage waveform in the test bench

case, the voltage curves are also measured on the LV side of the DUT transformer. Figure 8 illustrates, how the voltages are transfered from the terminal of grid emulator through the transformers towards the measurement point at the DUT. At the grid-emulator terminals, the simulated unsymmetrical grid fault results in a voltage constellation type D according to [8]. The vectorial sum of the three-phase voltage vectors remain 0 since the grid emulator is not able to apply any zero-sequence voltages.

Due to the winding configuration of grid emulator transformer, the voltage vector constellation is transformed on the PCC side into fault type C according to [8]. Fault type C reflects a fault case where two phases are involved. Thus, only two phase vectors are affected while the other vector remains unchanged. On the LV side of the DUT transformer, a fault type D is obtained, since the transformer is constructed with the same winding configuration as the grid emulator transformer.

It can be concluded that single-phase grid faults cannot be generated at the PCC. However, the capability of the grid emulator already covers the necessary fault types to be tested according to the standard IEC 61400-21 and the test guidelines FGW TR 3 [9].

To demonstrates the emulation of grid-fault events on the test bench and to observe the reaction of the currently installed DUT while a grid-fault occurs, several fault scenarios are emulated. Figure 9 presents the behavior of the DUT during an $80\,\%$ symmetrical voltage dip. In Fig. 9(a) the characteristic of the rms voltage is shown during the voltage dip. The behavior of the DUT during this event is plotted in Fig. 9(b). Each converter is loaded with approximately $19\,\%$ of its nominal power while the test is performed.

The grid-fault is indicated by the decay of the voltage curve starting at $t = 1\,\mathrm{s}$. As can be observed, the DUT starts reacting and increases the current once the voltage falls below $90\,\%$ of the nominal voltage. Firstly, the active current is increased inversely proportional to the voltage drop to keep the supplied active power into the grid as constant as possible. Secondly, the reactive current is enhanced to avoid a further voltage drop as requested by the grid code [7]. Within a voltage band between $90\,\%$ and $100\,\%$ of the nominal voltage, no additional reactive current from DUT is demanded.

The magnitude of the additional reactive current injected by the DUT ($\Delta I_{\mathrm{reactive}}$) is characterized by a multiplication factor k as described in [7]. To determine the requested $\Delta I_{\mathrm{reactive}}$ by the grid operator for a specific voltage dip, the factor k is multiplied by the difference between the dip voltage and the dead-band voltage of $90\,\%$. Taking the emulated fault event as an example, an $80\,\%$ dip voltage will result in $\Delta I_{\mathrm{reactive}} = 20\,\%$ with $k = 2$. k must be coordinated with the grid operator before integrating the wind turbines to the grid.

As it can be observed in Fig. 9(b), the measured reactive current supplied by the DUT does not reach the requested value of $20\,\%$ according to $k = 2$. Due to the impedance between the grid emulator and the measurement point, the voltage shows an increase while the DUT the current feed-in. This reaction of the emulated grid forces the DUT to reduce the $\Delta I_{\mathrm{reactive}}$ accordingly. Finally, a $\Delta I_{\mathrm{reactive}}$ of about $15\,\%$ is

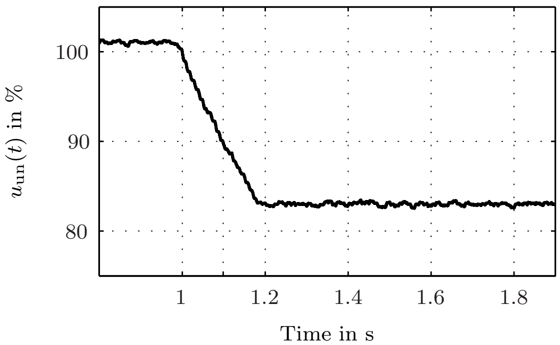

(a) Grid rms-voltage

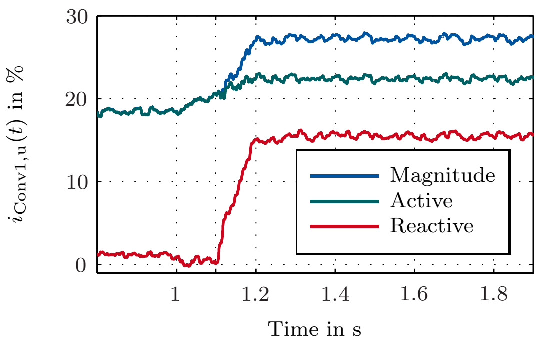

(b) Effective current of one DUT converter

Fig. 9. Behavior of the DUT during grid fault

obtained at the stable operation. Such a reaction of grid voltage may also be observed in reality depending on the characteristic of the grid impedance at the PCC.

VI. Efficiency Measurement

To further demonstrate the capabilities and advantages of the $4\,\mathrm{MW}$ test-bench, an efficiency measurement is performed on the generator of Winergy's HybridDrive. The efficiency is calculated as the ratio between the mechanical input power and the electrical output power, for different torque and speed steps.

In order to determine the mechanical power, the torque is measured at the interface between the gearbox and the generator of the HybridDrive (at the medium-speed shaft). The speed is measured at the end of the generator shaft. The HybridDrive generator is equipped with three parallel-connected three-phase winding systems, each connected to the grid via a power electronics converter. In a first step, the symmetry of each winding system is verified. Then, single-phase power measurements are performed for each converter in order to verify their symmetrical power loading. The total electrical power of the HybridDrive generator is calculated based on the single-phase power measured for each winding system.

The hereby determined efficiencies of the HybridDrive generator are subsequently transferred on a wind speed characteristic, which is based on the power curve of a $3\,\mathrm{MW}$ W2E wind turbine [10]. As shown in Fig. 10, all points are measured during partial-load operation and a maximum efficiency of $96.2\,\%$ is recorded. During full-load operation (for

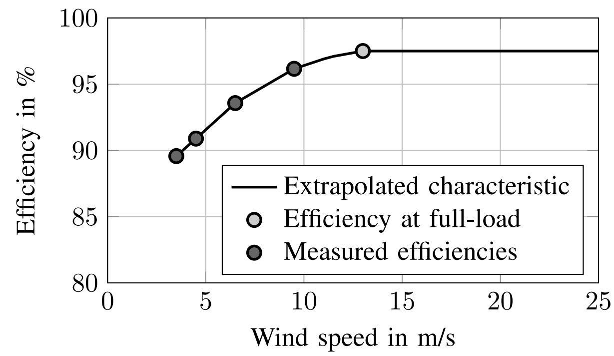

Fig. 10. Efficiency of Winergy's HybridDrive generator.

wind speeds above $13\,\mathrm{m/s}$), where the generator of Winergy's HybridDrive has already reached its rated speed, an efficiency of $97.5\,\%$ is expected.

VII. Conclusions

In this paper, the developed of a $4\,\mathrm{MW}$ full-size wind-turbine test bench is presented. With the current setup of the grid emulator, a synchronous operation of the installed DUT is possible without any significant negative interactions with the grid emulator. This enables an application of load scenarios to the DUT for further observation of the operation behavior. Also, the efficiency of DUT can be estimated. It can be concluded that this test bench can improve the development process of future wind turbine systems.

Acknowledgment

The authors would like to thank the EFRE (NRW Ziel 2-Programm 2007-2013) for the financial support of this work. The authors would also like to thank Winergy for providing the device-under-test.

References

[1] A. Helmedag, T. Isermann, A. Monti, N. Averous, M. Stieneker, and R. De Doncker, "Multi-physics power hardware in the loop test bench for on-shore wind turbine nacelles," in *ECCE Asia Downunder (ECCE Asia), 2013 IEEE*, June 2013, pp. 221–226.

[2] A. Nabae, I. Takahashi, and H. Akagi, "A new neutral-point-clamped pwm inverter," *Industry Applications, IEEE Transactions on*, vol. IA-17, no. 5, pp. 518–523, Sept 1981.

[3] DIN, *EN 50160 - Merkmale der Spannung in oeffentlichen Elektrizittsversorgungsnetzen*, DIN Std. DIN EN 50 160:2011-02, 2011.

[4] Winergy. (2015) Hybriddrive. [Online]. Available: www.winergy-group.com

[5] IEC, *Wind turbines - Part 21: Measurement and assessment of power quality characteristics of grid connected wind turbines*, IEC Std. 61 400-21, 2008.

[6] BDEW, *Technical Guideline Generating Plants Connected to the Medium Voltage Network*, June 2008.

[7] *Verordnung zu Systemdienstleistung durch Windenergieanlagen (Systemdienstleistungsverordnung - SDLWindV)*, Std., July 2009. [Online]. Available: www.bundesgesetzblatt.de

[8] M. H. Bollen, *Understanding Power Quality Problems: Voltage Sags and Interruptions*. Wiley, 2000.

[9] FGW, *TR 3: Bestimmung der elektrischen Eigenschaften von Erzeugungseinheiten am Mittel-, Hoch- und Hchstspannungsnetz*, March 2010.

[10] W2E Wind to Energy. (2015, April) W2E 3.0 MW. [Online]. Available: http://www.w2e-rostock.de/fileadmin/user_upload/download/2014w2e_data-sheet-3000_web.pdf